Involvement of Inflammatory Chemokines in Survival of Human Monocytes Fed with Malarial Pigment[▽]

Giuliana Giribaldi,[1]*§ Mauro Prato,[1]§ Daniela Ulliers,[1] Valentina Gallo,[1] Evelin Schwarzer,[1]
Oskar B. Akide-Ndunge,[1] Elena Valente,[1] Silvia Saviozzi,[2]
Raffaele A. Calogero,[2] and Paolo Arese[1]

*Department of Genetics, Biology and Biochemistry, University of Torino Medical School, Turin, Italy,[1] and Department of
Clinical and Biological Sciences, University of Torino, San Luigi Hospital, Orbassano, Turin, Italy[2]*

Hemozoin (HZ)-fed monocytes are exposed to strong oxidative stress, releasing large amounts of peroxidation derivatives with subsequent impairment of numerous functions and overproduction of proinflammatory cytokines. However, the histopathology at autopsy of tissues from patients with severe malaria showed abundant HZ in Kupffer cells and other tissue macrophages, suggesting that functional impairment and cytokine production are not accompanied by cell death. The aim of the present study was to clarify the role of HZ in cell survival, focusing on the qualitative and temporal expression patterns of proinflammatory and antiapoptotic molecules. Immunocytochemical and flow cytometric analyses showed that the long-term viability of human monocytes was unaffected by HZ. Short-term analysis by macroarray of a complete panel of cytokines and real-time reverse transcription (RT)-PCR experiments showed that HZ immediately induced interleukin-1β (IL-1β) gene expression, followed by transcription of eight additional chemokines (IL-8, epithelial cell-derived neutrophil-activating peptide 78 [ENA-78], growth-regulated oncogene α [GROα], GROβ, GROγ, macrophage inflammatory protein 1α [MIP-1α], MIP-1β, and monocyte chemoattractant protein 1 [MCP-1]), two cytokines (tumor necrosis factor alpha [TNF-α] and IL-1receptor antagonist [IL-1RA]), and the cytokine/chemokine-related proteolytic enzyme matrix metalloproteinase 9 (MMP-9). Furthermore, real-time RT-PCR showed that 15-HETE, a potent lipoperoxidation derivative generated by HZ through heme catalysis, recapitulated the effects of HZ on the expression of four of the chemokines. Intermediate-term investigation by Western blotting showed that HZ increased expression of HSP27, a chemokine-related protein with antiapoptotic properties. Taken together, the present data suggest that apoptosis of HZ-fed monocytes is prevented through a cascade involving 15-HETE-mediated upregulation of IL-1β transcription, rapidly sustained by chemokine, TNF-α, MMP-9, and IL-1RA transcription and upregulation of HSP27 protein expression.

Plasmodium falciparum is an intracellular parasite that is responsible for the most serious form of malaria. This protozoan survives within erythrocytes, using hemoglobin as a protein source and generating ferriprotoporphyrin IX crystal hemozoin (HZ) (malarial pigment) as a waste product. HZ is avidly phagocytosed and persists undigested in human monocytes, seriously compromising several functions, such as repeated phagocytosis (54), antigen presentation (53, 58, 59), oxidative burst (58), bacterial killing (8), differentiation/maturation into dendritic cells (63), and coordination of erythropoiesis (17). Nevertheless, studies performed in patients with severe malaria have shown the abundant presence of HZ-loaded circulating monocytes and tissue/organ macrophages (1, 13, 36), indicating that their functional impairments and cytokine production do not induce apoptosis. Clearance of apoptotic cells from inflammatory sites is an important mechanism that prevents exposure of tissues to noxious contents released by inflammatory cells and enables the resolution of inflammation and healing (4). It is commonly accepted that

monocyte viability is influenced by previous inflammatory responses (reviewed in reference 9). Moreover, HZ-fed monocytes have been shown to produce large amounts of cytokines, such as tumor necrosis factor alpha (TNF-α) and interleukin-1β (IL-1β) (44), and to enhance the expression, release, and activity of the cytokine-dependent molecule matrix metalloproteinase 9 (MMP-9) (48, 49). However, the complete profile and temporal pattern of native HZ-induced cytokine and cytokine-related molecule gene expression is still missing.

By heme catalysis, HZ-fed human monocytes generate large amounts of peroxidation products of polyunsaturated fatty acids (PUFAs), such as hydroxyeicosatetraenoic acids (HETEs), hydroxyoctadecadienoic acids (HODEs), and the terminal aldehyde 4-hydroxynonenal (HNE) (55). Lipid derivatives are possible inducers of the effects of HZ on inflammatory molecules; indeed, it has been demonstrated that 15-HETE mimics the effects of HZ on IL-1β, TNF-α, and MMP-9 production (45, 46) and causes similar changes in gene expression (52). Both cytokines and oxidative stress have the potential to regulate the expression of heat shock proteins (HSPs), a well-conserved family of chaperones also strongly induced by heat, irradiation, or anticancer chemotherapy (reviewed in references 11 and 35). HSPs play an important role in apoptosis regulation, functioning as chaperones for denatured proteins; more specifically, HSP27 has cytoprotective functions and in-

hibits key effectors of the apoptotic machinery at the pre- and postmitochondrial levels (reviewed in references 5 and 70).

To clarify the role of HZ in cell survival, it may be useful to obtain a broader picture of the molecules induced by HZ, as they are potential targets for more focused antimalarial therapy. Here, we show by immunocytochemistry and fluorescence-activated cell sorter (FACS) analysis that HZ-fed monocytes exhibit prolonged cell viability (up to 72 h), and we correlate cell survival with 15-HETE-mediated transcription of IL-1β, rapidly followed by enhanced expression of the chemokines TNF-α, MMP-9, and IL-1receptor antagonist [IL-1RA] and upregulation of HSP27.

MATERIALS AND METHODS

Materials. Unless otherwise stated, reagents were obtained from Sigma-Aldrich, St. Louis, MO. Sterile plastics were from Costar, Cambridge, United Kingdom; Panserin 601 monocyte medium was from PAN Biotech, Aidenbach, Germany; percoll was from Pharmacia, Uppsala, Sweden; Dynabeads M-450 CD2 Pan T and M-450 CD19 Pan B were from Dynal, Oslo, Norway; Diff-Quik parasite stain was from Baxter Dade AG, Dudingen, Switzerland; 15-HETE was from Cayman, Ann Arbor, MI; the RNeasy Mini Kit was from Qiagen, Crawley, United Kingdom; the DNA-free kit was from Ambion, Austin, TX; the Panorama cDNA Labeling and Hybridization Kit and Panorama Human Cytokine Gene Arrays were from Sigma-Genosys, St. Louis, MO; the enhanced chemiluminescence (ECL) kit, $[\alpha^{-33}P]$dCTP, and horseradish peroxidase (HRP)-conjugated anti-mouse and anti-rabbit secondary antibodies were from GE Healthcare, Milan, Italy; RNasin was from Promega, Milan, Italy; the PhosphorImager Screen, PhosphorImager Storm 860, and ImageQuant 5.0 software were from Molecular Dynamics, Sunnyvale, CA; avian myeloblastosis virus (AMV), Moloney murine leukemia virus (MMLV), oligo(dT), and primers for real-time reverse transcription (RT)-PCR were from Invitrogen Life Technologies, Carlsbad, CA; deoxynucleoside triphosphates (dNTPs) were from Applied Biosystems, Foster City, CA; IQ SYBR green Supermix, the iCycler instrument for real-time RT-PCR, the Geldoc computerized densitometer, and electrophoresis reagents were from Bio-Rad Laboratories, Hercules, CA; Beacon Designer 7.0 software was from Premier Biosoft International, Palo Alto, CA; the ApopTag in Situ Apoptosis Detection Kit was from Oncor, Eastleigh, United Kingdom; the TACS Annexin Kit for apoptosis detection by flow cytometry was from Trevigen, Gaithersburg, MD; the FACSCalibur cytometer and Cell Quest software were from BD Biosciences, San Jose, CA; the bicinchoninic acid protein assay was from Pierce, Rockford, IL; the anti-HSP27 polyclonal antibody (Ab) was from Stressgen, Ann Arbor, MI; and Mayer's hemallume was from Kaltek srl, Padova, Italy.

Culturing of _P. falciparum_ and isolation of native HZ and dHZ. _P. falciparum_ parasites (Palo Alto strain; mycoplasma free) were kept in culture as described previously (16). After centrifugation at $5,000 \times g$ on a discontinuous Percoll-mannitol density gradient (16), HZ was collected from the 0-to-40% interphase, washed five times with 10 mM HEPES (pH 8.0) containing 10 mM mannitol at 4°C and once with phosphate-buffered saline (PBS), and stored at 20% (vol/vol) in PBS at −20°C or immediately used for opsonization and phagocytosis. For delipidized HZ (dHZ), lipid extraction was performed as previously reported (46).

Isolation of monocytes. Human monocytes were separated from freshly collected buffy coats (discarded from blood donations by healthy adult donors of both sexes) provided by the local blood bank (Associazione Volontari Italiani Sangue [AVIS], Turin, Italy) by Ficoll centrifugation and lymphocyte depletion with PanT/PanB-Dynal beads as described previously (49). Two milliliters of monocytes, resuspended at 1.25×10^6 cells per milliliter of RPMI 1640 medium, was plated in 35-mm-diameter culture dishes. After a 1 h-incubation in a humidified CO$_2$/air incubator at 37°C, the dishes were washed three times with RPMI 1640 to remove nonadherent cells. Two milliliters of Panserin 601 medium was added to each dish, and the cells were cultured overnight. The Panserin medium was then removed, and 2 ml of RPMI 1640 was added to each dish before phagocytosis was started. In experiments of apoptosis detection by immunocytochemical staining, after isolation, monocytes were plated at 2×10^6 to 4×10^6 cells/plastic coverslip and treated as described above.

Phagocytosis of opsonized HZ, dHZ, and latex beads. HZ/dHZ, washed once and finely dispersed at 30% (vol/vol) in PBS, and latex beads (0.114-μm diameter) suspended at 5% (vol/vol) in RPMI 1640 were added to the same volume of fresh human AB serum (AVIS blood bank) and incubated for 30 min at 37°C as described previously (49). Phagocytosis was started by adding to the adherent monocytes opsonized HZ/dHZ (50 red blood cell [RBC] equivalents of heme content per monocyte) and latex beads (10 μl of a 100-fold dilution of the opsonized latex bead suspension per 10^6 monocytes). After 2 h, phagocytosis was stopped by three washings with RPMI 1640. The amount of HZ phagocytosed by monocytes was quantified by luminescence as described previously (57, 58); on average, each monocyte ingested HZ equivalent to ∼8 to 10 trophozoites, in terms of ingested heme. The plates were then incubated in Panserin 601 medium in a humidified CO$_2$/air incubator at 37°C for the indicated times (0, 2, or 4 h for gene expression studies; 9 h for HSP protein expression analysis; 24 to 72 h for apoptosis detection). Under certain conditions for selected experiments, unfed monocytes were incubated as follows: with 1 μg/ml lipopolysaccharide (LPS) for 4 to 6 h (macroarray assay), with 10 μM 15-HETE for 6 h (real-time RT-PCR studies), and with 10 μM gliotoxin for 9 h (apoptosis detection and studies on HSP modulation).

Apoptosis detection by immunocytochemical staining and flow cytometry. After termination of 2 h of phagocytosis, the monocytes were further incubated with Panserin 601 monocyte medium in a humidified CO$_2$/air incubator at 37°C for 24 h (immunocytochemistry studies) or 72 h (flow cytometry studies). Alternatively, to obtain a positive control for apoptosis, monocytes were incubated with 10 μM gliotoxin for 6 h. Thereafter, monocytes adherent to coverslips were fixed in 4% (vol/vol) neutral buffered formalin for 10 min at room temperature. DNA fragmentation was determined using the ApopTag in Situ Apoptosis Detection Kit, according to the manufacturer's instructions. Briefly, the coverslips were equilibrated in equilibration buffer for 30 min and incubated with 54 μl of Working Strength TdT Enzyme (ApopTag kit) (for terminal deoxynucleotidyl transferase-mediated addition of digoxigenin-nucleotides to DNA). The reaction was blocked by transferring specimens to a Coplin jar containing Working Strength Stop/wash buffer (ApopTag kit). The incorporated nucleotides formed a random heteropolymer of digoxigenin-11–dUTP and dATP, detected with peroxidase-conjugated anti-digoxigenin antibody. The coverslips were then incubated in 0.05% (wt/vol) diaminobenzidine in PBS with 0.02% (vol/vol) hydrogen peroxide. Specimens were washed with water, counterstained with Mayer's hemallume for a few minutes, and then rinsed, dehydrated, and mounted for microscope analysis. Alternatively, monocyte apoptosis was evaluated by flow cytometry using fluorescein isothiocyanate (FITC)-conjugated annexin V and propidium iodide staining (TACS Annexin Kit), according to the manufacturer's instructions. Briefly, cells were washed with PBS with Ca^{2+} and then incubated for 15 min at 25°C with 0.025 μg FITC-conjugated annexin V and 0.5 μg propidium iodide before analysis with a FACSCalibur cytometer, using Cell Quest software. Live cells were distinguished from apoptotic or necrotic cells by appropriately gated light scatter characteristics. A total of 30,000 events were collected for each sample. Data analysis was performed with WinMDI software.

RNA isolation. After 2 h of phagocytosis, monocytes were incubated with Panserin 601 monocyte medium in a humidified CO$_2$/air incubator at 37°C for 0, 2, and 4 h. Total RNA was isolated from 15×10^6 monocytes using an RNeasy Mini Kit in accordance with the manufacturer's instructions. A DNA digestion step with the DNA-free kit was included to avoid any genomic DNA contamination. In a typical experiment, 15×10^6 monocytes yielded 4 to 8 μg of RNA.

Preparation of ^{33}P-radiolabeled probes. ^{33}P-radiolabeled cDNA probes for array hybridization were prepared by reverse transcription. A Panorama cDNA Labeling and Hybridization Kit was used. To a solution of 2 μg of RNA in 7 μl of diethyl pyrocarbonate (DEPC)-treated water, 4 μl of human cytokine cDNA labeling primers were added. After incubation for 2 min at 75°C in a heating block, the solution was cooled to 42°C and then added to 6 μl of 5× reverse transcription buffer, 3 μl of dNTP mixture (10 mM [each] dATP, dGTP, and dTTP), 0.5 μl of dCTP (100 μM), 7 μl of 10 μCi/μl $[\alpha^{-33}P]$dCTP (2,000 to 3,000 Ci/mmol), 0.5 μl of 40 U/μl RNasin (RNase inhibitor), and 2 μl of 25 U/μl AMV reverse transcriptase. Following 3 h of incubation at 42°C, the probes were purified by passage through Sephadex G-25 spin columns.

Human cDNA expression arrays. Panorama Human Cytokine Gene Arrays consisted of a matched set of charged nylon membranes containing PCR products spotted in duplicate. Each array contained 375 different human cytokine-related genes. Hybridization was carried out according to the manufacturer's instructions. Briefly, ^{33}P-radiolabeled first-strand cDNA probes were prepared as described above, and the arrays were prehybridized for 1 h at 65°C in hybridization solution (from the Panorama cDNA Labeling and Hybridization Kit). Filters were then incubated with the denatured, labeled cDNA for 15 h at 65°C in a hybridization oven. The filters were washed extensively under low- and high-stringency conditions in hybridization bottles and exposed to a phosphorimager screen for 24 h at 4°C, and the resulting hybridization signals were quantified using a PhosphorImager Storm 860 and ImageQuant 5.0 software.

TABLE 1. SYBR-Green real-time RT-PCR primers and conditions

Protein[a]	Primer concn (nM)	T_a[b] (°C)	Efficiency (%)	Sequence (5′–3′)	PCR product	
					Length (bp)	T_m[c] (°C)
ENA-78 (X78686)	300	60	81.5	CGTGTCCCCGGTCCTTCGAG CTCAACACAGCAGCGGCAGG	107	94.2
GROα (J03561)	300	60	89.8	GCTTGCCTCAATCCTGCATCCC CCAGTGAGCTTCCTCCTCCCTTC	101	83.7
GROβ (M36820)	300	60	90.6	TGTCTCAACCCCGCATCGC TTCAGGAACAGCCACCAATAAGC	112	84.7
GROγ (M36821)	F, 600; R, 900[d]	60	90.3	ACTGAACAAGGGGAGCACCAACTG CAGCTCTGGTAAGGGCAGGGAC	100	85.6
IL-8 (Y00787)	300	60	89.6	CTGGCCGTGGCTCTCTTGG GGGTGGAAAGGTTTGGAGTATGTC	125	86.5
MCP-1 (S69738)	300	60	103.7	AGAATCACCAGCAGCAAGTGTCC ATGGAATCCTGAACCCACTTCTGC	104	86
MIP-1α (NM_002983)	300	60	94.7	CATCACTTGCTGCTGACACG TGTGGAATCTGCCGGGAG	64	86
MIP-1β (J04130)	300	60	99.6	TAGTAGCTGCCTTCTGCTCTCCAG TCTACCACAAAGTTGCGAGGAAGC	112	89.4
IL-1β (NM_000576)	300	60	90.5	ACAGATGAAGTGCTCCTTCCA GTCGGAGATTCGTAGCTGGAT	73	85.7
TNF-α (M10988)	300	60	87.1	AGCCTCTTCTCCTTCCTGATCGTG GGCTGATTAGAGAGAGGTCCCTGG	115	91.2
IL-1RA (NM_000577)	900	60	90.3	GAAGATGTGCCTGTCCTGTGT CGCTCAGGTCAGTGATGTTAA	80	83.9
MMP-9 (NM_004994)	300	57	99.7	CCTGGAGACCTGAGAACCAATC CTCTGCCACCCGAGTGTAAC	84	85.8
GAPDH (BC020308)	300	60	94.2	GAAGGTGAAGGTCGGAGT CATGGGTGGAATCATATTGGAA	155	86.5

[a] Accession numbers are in parentheses.
[b] T_a, annealing temperature.
[c] T_m, melting temperature.
[d] F, forward; R, reverse.

The intensity of each spot was corrected for background levels and normalized for differences in probe labeling using the average values for all genes. Genes showing a change of $\geq$1.5-fold in intensity were considered to be upregulated following phagocytosis.

Real-time RT-PCR studies. RNA (2 μg) was reverse transcribed into single-stranded cDNA using MMLV (200-U/μl final concentration) and oligo(dT) (25-μg/μl final concentration). The real-time RT-PCR experiments were performed on the iCycler instrument. The specific primers were designed with the Beacon Designer Software package (Table 1 shows the complete list). Oligonucleotide sequences were designed to be intron spanning, allowing differentiation between cDNA- and DNA-derived PCR products. Real-time RT-PCR assays were performed in a final volume of 25 μl containing 2 μl of cDNA diluted 1:5, primer pair concentrations as indicated in Table 1, and 12.5 μl of IQ SYBR green Supermix. DNA polymerase was preactivated for 2 min at 95°C, and amplification was performed with a 45-cycle PCR (94°C for 30 s, annealing temperature as indicated in Table 1 for 30 s, and 72°C for 30 s). The GAPDH (glyceraldehyde-3-phosphate dehydrogenase) gene was used as a housekeeping gene (primer sequences were from the Bio-Rad library). For quantification of the PCR results, expressed as fold variation over control (untreated cells), the efficiency-corrected quantification model was used (43). The C_T values were means of triplicate measurements. To validate the method, serial dilutions of cDNA from monocytes, stimulated for 6 h with LPS, were tested. The analyzed transcripts exhibited high-linearity amplification plots ($r > 0.98$) and similar PCR efficiencies (see Table 1), confirming that the expression levels of the genes could be directly compared to one another. The specificity of PCR was confirmed by melt curve analysis. The melting temperatures for each amplification product are expressed in Table 1.

Anti-HSP27 and anti-HSP70 Western blotting. After 2 h of phagocytosis, monocytes were further incubated with Panserin 601 monocyte medium in a humidified CO_2/air incubator at 37°C for 9 h. Subsequently, the cells were washed and lysed at 4°C in lysis buffer containing 300 mM NaCl, 50 mM Tris, 1% (vol/vol) Triton X-100, and protease and phosphatase inhibitors (50 ng/ml pepstatin, 50 ng/ml leupeptin, and 10 μg/ml aprotinin). The protein content of the lysate was measured by a bicinchoninic acid assay. Lysate samples (25 μg protein/

lane) were separated by electrophoresis on 8% and 12% polyacrylamide gels under denaturing and reducing conditions, with addition of Laemmli buffer (100 mM Tris-HCl, pH 6.8, 2% [wt/vol] SDS, 20% [vol/vol] glycerol, 4% [vol/vol] β-mercaptoethanol) (28), blotted on a polyvinylidene difluoride membrane, and probed with 1:5,000 polyclonal rabbit anti-HSP27 and 1:2,000 monoclonal anti-HSP70 antibodies. After 5-min washes, the blot was incubated for 1 h with a 1:10,000 dilution of anti-rabbit or anti-mouse IgG horseradish peroxidase-labeled antibody, and immunoreactivity was detected with an ECL kit. Band densitometric analysis was performed using a Geldoc computerized densitometer.

Statistical analysis. For macroarray experiments, 2 array gene filters for each experimental condition were hybridized with ^{33}P-labeled cDNA synthesized from 2 different pools of RNA, each obtained from monocytes from 3 different donors (total number of donors, 6). All other data were obtained from three independent experiments with similar results. The results are shown as means plus standard errors of the mean (SEM) or as representative images. All data were analyzed by Student's t test, except those obtained from experiments with 15-HETE, which were analyzed by a one-way analysis of variance (ANOVA) and Tukey's test. A P value of <0.05 was considered significant.

RESULTS

Phagocytosis of HZ does not induce apoptosis in immuno-purified human monocytes. Apoptosis was studied by immunocytochemical staining of digoxigenin-labeled genomic DNA in 24-h-incubated unstimulated (Fig. 1A), 9-h gliotoxin-treated (Fig. 1B), and 24-h HZ-loaded (Fig. 1C) immunopurified monocytes. DNA fragmentation (brown cells) was rarely detected in unstimulated or HZ-fed monocytes (Fig. 1A and C), while it was clearly evident after 9 h in gliotoxin-treated monocytes (Fig. 1B). The absence of apoptosis after phagocytosis of
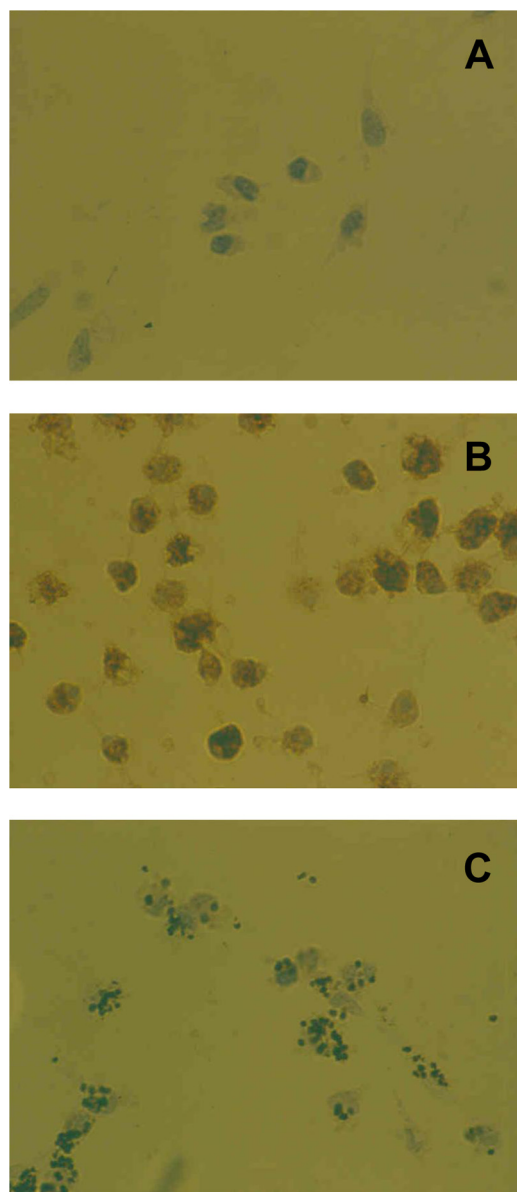
FIG. 1. Lack of short-term apoptosis in HZ-fed human monocytes. Immunopurified monocytes were incubated for 24 h following incubation with and without HZ and phagocytosis. Alternatively, cells were treated with 1 μM gliotoxin for 9 h. DNA fragmentation of immunopurified monocytes was detected by peroxidase immunocytochemical staining (brown). (A and C) Control (A) and HZ-fed (C) monocytes showed weak positivity with anti-digoxigenin antibody, indicating a predominantly poor DNA fragmentation. (B) Gliotoxin-treated monocytes were strongly positive with anti-digoxigenin antibody, indicating extensive DNA fragmentation. Representative images from three independent experiments are shown.

HZ was confirmed up to 72 h after phagocytosis, as shown by viability studies performed through FACS analysis (Table 2). On average, apoptosis was detected in <4% of unfed and HZ-fed monocytes, necrosis was <6% under both conditions, and viable cells were ~90% of total monocytes. Cells treated with gliotoxin showed 67.4% apoptosis, 11.7% necrosis, and 20.8% survival.

HZ modifies the expression of many genes in immunopurified human monocytes. Immunopurified monocytes were allowed to phagocytose HZ and latex particles (control meal) for 2 h and were further monitored at 0, 2, and 4 h after the end of the phagocytic period. As a positive control, we used cells treated with LPS for 2, 4, and 6 h. The cells were then exposed to macroarray analysis. Figure 2 shows two representative images of macroarrays obtained from unstimulated monocytes (Fig. 2A) and monocytes fed with HZ for 2 h and further incubated for 4 h (Fig. 2B). Fifteen genes were upregulated by HZ phagocytosis: 9 chemokines (interleukin 8 [IL-8], epithelial cell-derived neutrophil-activating peptide 78 [ENA-78], growth-regulated oncogene α [GROα], GRO-β, GRO-γ, monocyte chemoattractant protein 1 [MCP-1], macrophage inflammatory protein 1α [MIP-1α], MIP-1β, and myeloid progenitor inhibitory factor 1 [MPIF-1]), 4 cytokines (IL-1β, TNF-α, IL-1receptor antagonist [IL-1RA], and granulocyte–colony-stimulating factor [G-CSF]), 1 receptor (urokinase-type plasminogen activator receptor [uPAR]), and 1 matrix metalloproteinase (MMP-9). Analysis of normalized signal intensities of hybridized spots corresponding to induced genes is presented in Fig. 3: only genes showing at least a 1.5-fold increase were considered to be upregulated. Samples obtained after shorter incubation times following 2 h of HZ phagocytosis (0 and 2 h) did not show any modulation of gene expression (data not shown), except for IL-1β, which was time dependently upregulated from 0 h up to 4 h after phagocytosis of HZ, as shown in Fig. 3A; quantitation of genes upregulated 4 h after the end of phagocytosis of HZ (see above) is presented in Fig. 3B. Latex-fed monocytes, compared to unstimulated cells, displayed a moderate and transient upregulation of a restricted set of genes (ENA78, GROβ, IL-8, MCP-1, IL-1β, and IL-1RA) 2 h after phagocytosis, which totally disappeared 4 h after the end of phagocytosis; on the other hand, LPS (positive control) strongly induced a larger gene set than HZ at all times considered (data not shown). To validate the macroarray data, real-time RT-PCR for all 15 genes induced 4 h after phagocytosis of HZ was performed on RNA extracts. This approach confirmed that 12 genes were upregulated (Fig. 4) while 3 genes (MPIF-1, G-CSF, and uPAR) did not appear to be upregulated by HZ (data not shown).

15-HETE induces the transcription of chemokine genes in immunopurified human monocytes. To assess if 15-HETE could play a role in HZ-dependent upregulation of genes previously identified by macroarray analysis, immunopurified monocytes were treated with 1 μM and 10 μM 15-HETE for 6 h. Ten micromolar is the dose of 15-HETE that a monocyte

TABLE 2. Long-term viability of HZ-fed human monocytes[a]

Cell condition	Unfed monocytes	Gliotoxin-treated monocytes	HZ-fed monocytes
Apoptosis	3.2 ± 0.9	67.4 ± 11.2	3.9 ± 0.3
Necrosis	5.1 ± 1.4	11.7 ± 1.5	6.0 ± 1.4
Alive	91.6 ± 1.2	20.8 ± 10.4	90.0 ± 1.5

[a] Data are expressed as mean percentage ± SEM of three independent experiments. The data were analyzed by Student's t test. HZ-fed versus unfed cells, not significant (all parameters); HZ-fed versus gliotoxin-treated cells, $P < 0.005$ (survival), $P < 0.005$ (apoptosis), and $P < 0.05$ (necrosis); unfed versus gliotoxin-treated cells, $P < 0.005$ (survival), $P < 0.005$ (apoptosis), and $P < 0.05$ (necrosis).
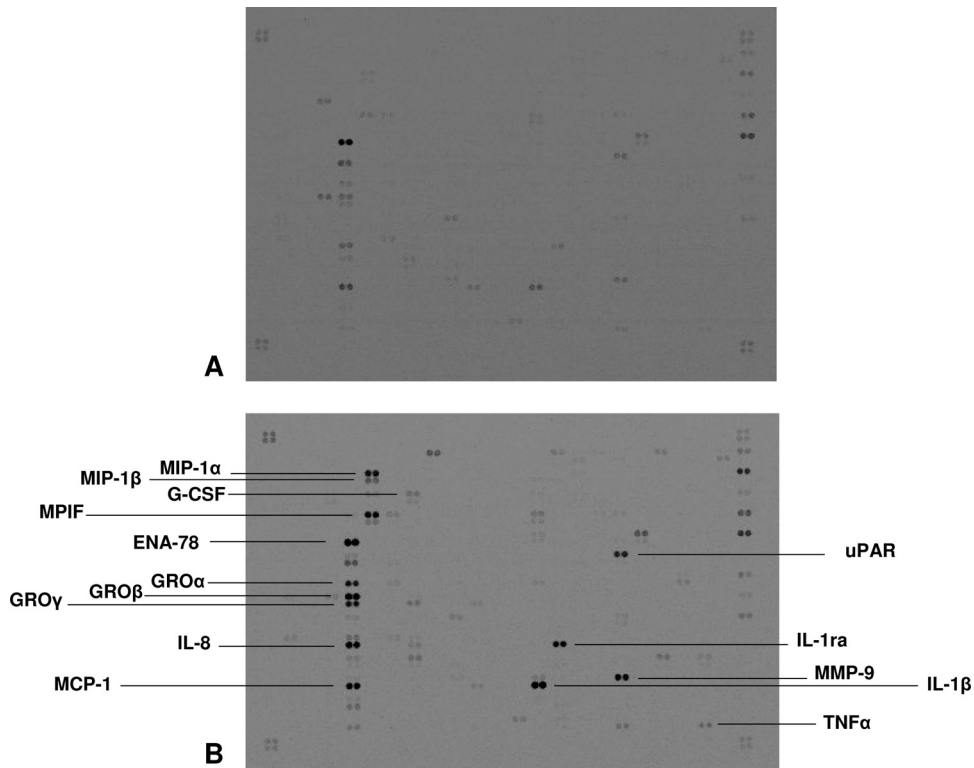
FIG. 2. Differential gene expression of unfed and HZ-fed human monocytes as measured by cDNA macroarray. Unfed (A) and HZ-fed (B) immunopurified human monocytes were incubated for 4 h following 2 h of phagocytosis. After isolation, the pooled RNAs of monocytes obtained from 3 different healthy blood donors were converted into ^{33}P-labeled cDNA probes. The probes were hybridized to a Panorama Human Cytokine Gene Array filter containing 375 different human cytokine-related genes spotted in duplicate. Hybridization was detected using a phosphorimager. The most strongly upregulated genes are labeled. The data were obtained from one representative of two independent experiments.

might engulf with HZ, under the realistic assumption of 10 RBC equivalents per monocyte and a monocyte volume of 500 fl (55). Real-time RT-PCR analysis for chemokine (Fig. 5A) and IL-1RA (Fig. 5B) genes showed that 1 μM 15-HETE did not induce any significant increase of gene expression, while a significant 2- to 3-fold increase was obtained with higher doses of 15-HETE for ENA-78, GROα, GROβ, and IL-8 genes. All other genes were not significantly modulated, although some
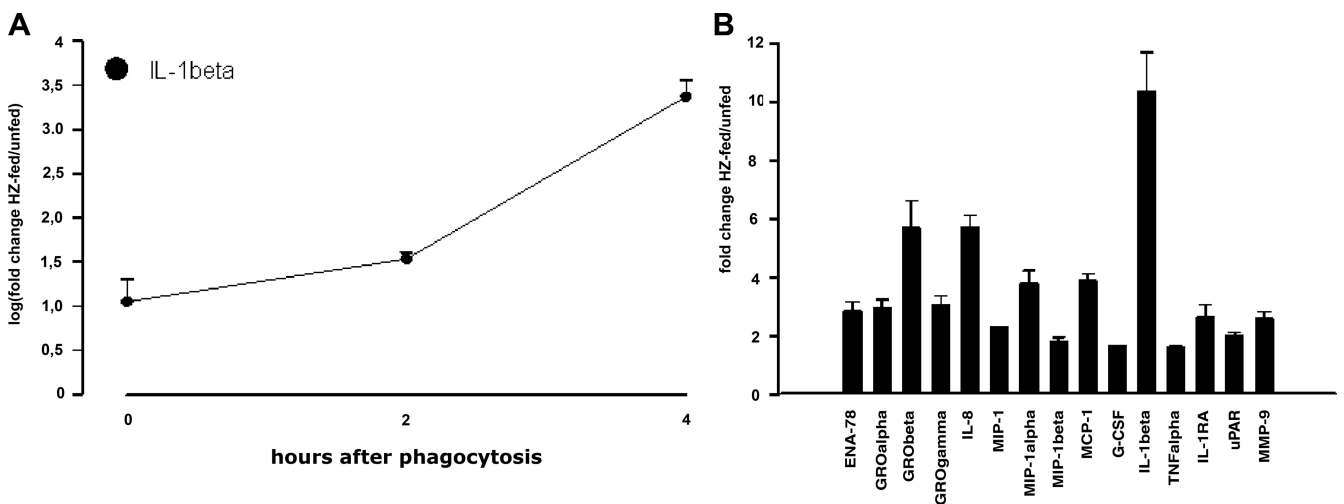

FIG. 3. Quantitation of relative upregulated genes in HZ-fed versus unfed human monocytes as determined from the ^{33}P-labeled phosphorimages. Differential gene expression in HZ-fed/unfed immunopurified human monocytes incubated for 0, 2, and 4 h after phagocytosis is shown. Genes showing a change of 1.5-fold or more in intensity were considered to be upregulated. The IL-1β gene was the only gene upregulated at all three times of incubation after phagocytosis of HZ (A), while 15 genes showed 1.5-fold or greater induction at the longest time of incubation (4 h) after the end of phagocytosis of HZ (B). The results are expressed as means plus SEM of two independent experiments. The changes in expression of the upregulated genes shown were statistically significant (worst P value, <0.05) compared to the average values of changes in expression for all genes.
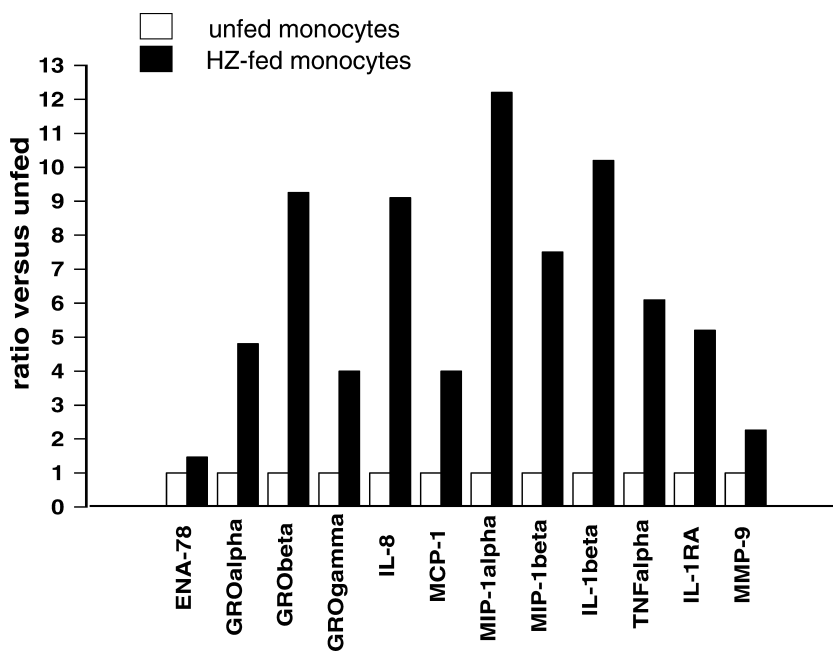
FIG. 4. Real-time RT-PCR validation of macroarray results. Unfed and HZ-fed immunopurified human monocytes were incubated for 4 h after phagocytosis. Threshold cycle values were normalized to GAPDH expression. The data are expressed as the ratio between relative gene expression levels of HZ-fed versus unfed monocytes and show only genes confirmed to be upregulated at least 1.5-fold. A representative experiment performed on the same pooled RNA utilized for the macroarray assay is shown.

increase was observed occasionally in separate experiments. Additional experiments performed on monocytes treated with dHZ suggested a major role for the crystal moiety of HZ in the upregulation of MCP-1 and MIP-1α, while for GROα, cooperation between lipid and crystal moieties is likely (not shown).

Phagocytosis of HZ enhances HSP27, but not HSP70, expression in immunopurified human monocytes. Expression of HSP27 and HSP70 proteins was studied by Western blotting and densitometric analysis in immunopurified, unstimulated, HZ-fed, and gliotoxin-treated monocytes after 9 h of incuba-
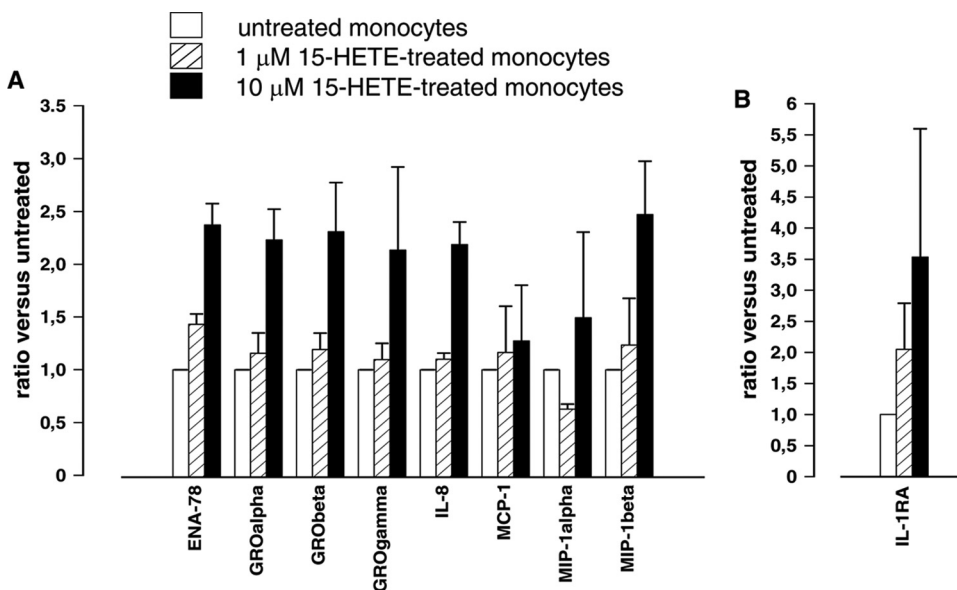

FIG. 5. Real-time RT-PCR analysis of HZ-related chemokines and IL-1RA gene expression in 15-HETE-treated human monocytes. Immunopurified monocytes were treated for 6 h with different doses of 15-HETE (1 μM and 10 μM). The expression of ENA-78, GROα, GROβ, GROγ, IL-8, MCP-1, MIP-1α, and MIP-1β (A) and IL-1RA (B) genes was measured. Threshold cycle values were normalized to GAPDH, and the data are expressed as the ratio between relative gene expression levels of HETE-treated versus untreated monocytes. Measurements were done in triplicate, and the data are presented as means plus SEM. A one-way ANOVA and Tukey's test were used for statistical analysis: 1 μM 15-HETE-treated versus untreated cells, no significant increase ($P > 0.05$); 10 μM 15-HETE-treated versus untreated cells, significant increases for ENA-78 ($P = 0.001$), GROα ($P = 0.012$), GROβ ($P = 0.040$), and IL-8 ($P = 0.001$); all other genes were not significantly modulated ($P > 0.05$).
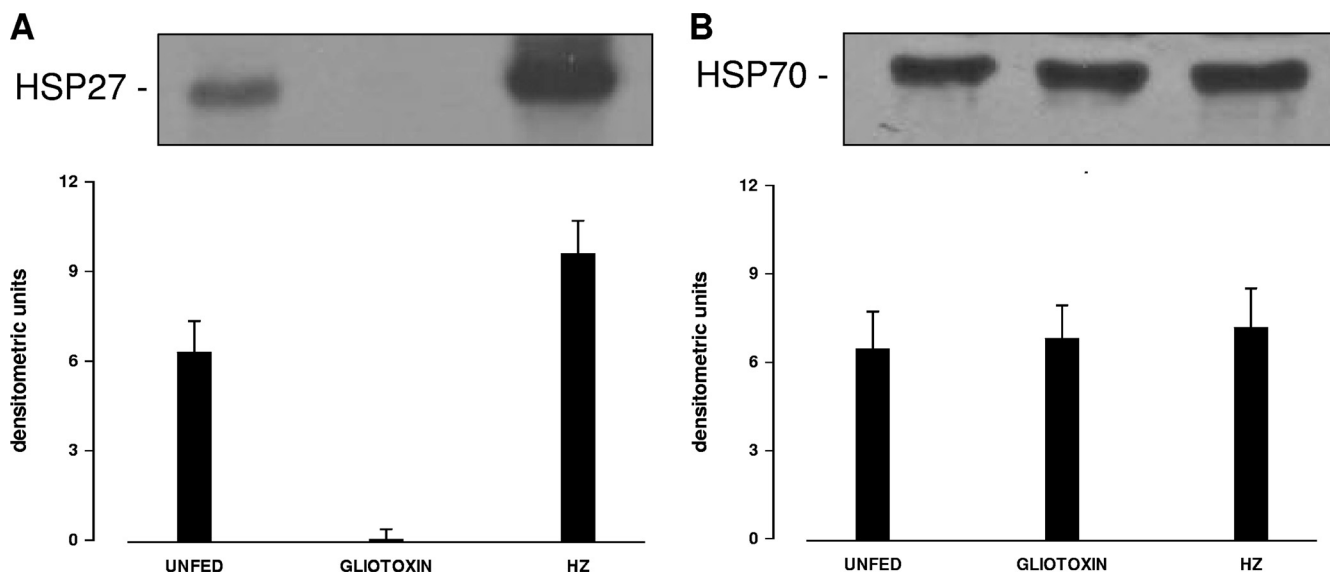
A

HSP27 -

B

HSP70 -

FIG. 6. Intermediate-term HSP27 and HSP70 protein expression in unfed and HZ-fed human immunopurified monocytes. Monocytes were incubated for 9 h following incubation with and without HZ and phagocytosis. Alternatively, cells were treated for 9 h with 1 μM gliotoxin. Thereafter, HSP27 (A) and HSP70 (B) proteins were detected in cell lysates by Western blotting (top; representative images) and analyzed by optical densitometry of 27- and 70-kDa bands (bottom; mean values plus SEM of arbitrary densitometric units from three independent experiments). The data were analyzed by Student's t test. (A) HZ-fed versus unfed cells, $P < 0.05$; gliotoxin-treated versus unfed cells, $P < 0.005$; HZ-fed versus gliotoxin-treated cells, $P < 0.002$. (B) No significant differences.

tion. As shown in Fig. 6A, HSP27 protein expression increased by 50% in HZ-fed monocytes versus unstimulated monocytes, while it was almost totally degraded after gliotoxin treatment. HSP70 was not significantly modulated (Fig. 6B).

DISCUSSION

Phagocytes, such as monocytes, are versatile cells that act as scavengers to rid the body of apoptotic and senescent cells and other debris through their phagocytic function. Although phagocytosis is a primary function of these cells, monocytes play vital roles in inflammation and repair of damaged tissues, secreting a large number of cytokines, chemokines, and growth factors that activate a variety of cell types and recruit them to inflamed tissue compartments. Since monocytes are important in regulating and resolving inflammation, their prolonged survival in tissue compartments could be detrimental. Thus, factors that regulate the fate of monocyte survival are important in cellular homeostasis (20). In malaria, circulating monocytes avidly phagocytose HZ, the heme detoxification biocrystal produced by the parasite during hemoglobin catabolism. HZ is not degraded by monocytes but persists for at least 72 h in the otherwise intact lysosomes of these cells (54, 56). As a consequence, numerous monocyte functions are impaired, including repeated phagocytosis (58), antigen presentation (59), oxidative burst (58), bacterial killing (8), maturation to dendritic cells (63), and coordination of erythropoiesis (17). Moreover, phagocytosis of HZ promotes cytokine production (44). Since the early 1980s, an adverse clinical course toward complicated malaria has been related to an unbalanced host immune response to *Plasmodium* infection, and a major role was suggested for excessive cytokines production by host cells (6), leading to several symptoms, such as hypoglycemia, hyperther-

mia, neurological manifestations, dyserythropoiesis, and immunodepression (7, 15, 18, 27, 40). In this context, a large amount of data for HZ-induced monocyte production of IL-1β and TNF-α (32, 44, 49, 60) is available; additionally, our laboratory previously described HZ-induced enhanced expression of MMP-9 (46, 49), an IL-1β- and TNF-α-inducible proteolytic enzyme able to disrupt the subendothelial basal lamina and cleave proforms of several molecules, including IL-1β and TNF-α themselves (see reference 38 for a review). The relationship among members of the HZ-dependent triad IL-1β/TNF-α/MMP-9 has been thoroughly investigated in recent years, and a model in which HZ first induces production of IL-1β, followed by TNF-α, has been proposed; in turn, both cytokines upregulate MMP-9 expression, release, and activity; finally, a long-term pathological autoenhanced loop between TNF-α and MMP-9 is established (46–49).

The present work shows that the viability of human monocytes is not affected by phagocytosis of HZ. Immunocytochemical and flow cytometric analyses performed at prolonged times (24 to 72 h) after phagocytosis of HZ showed that the survival rate of HZ-fed monocytes was similar to that of unfed monocytes. To better understand the mechanisms leading to survival of impaired HZ-fed monocytes during malaria, our study aimed first to expand knowledge of the array of molecules involved in the early inflammatory response to phagocytosed HZ by determining a complete profile of inflammatory gene expression in human monocytes and by investigating the role of 15-HETE, a potent lipoperoxidation product of HZ, in this response. In addition, as antiapoptotic HSP molecules are known to be induced by inflammation and oxidative stress (see references 5 and 70 for reviews), their role in the prevention of HZ-fed monocyte apoptosis was investigated.

Results obtained by PCR-validated macroarray screening

for short-term (0 to 4 h after phagocytosis) transcription of 375 inflammatory genes in HZ-fed immunopurified human monocytes not only confirmed previous observations of IL-1β, TNF-α, and MMP-9, but also showed HZ-dependent upregulation of additional molecules. The early inflammatory response to HZ was first triggered by enhanced IL-1β transcription 0 to 2 h after HZ phagocytosis ended and then reinforced (4 h after phagocytosis) by increased expression of MMP-9, TNF-α, and IL-1RA, a cytokine that was recently connected to increased severity of cerebral malaria (CM) (25). At this time, either macroarray analysis or real-time RT-PCR also detected enhanced expression of several molecules belonging to the chemokine class, a vast family of chemoattractant molecules involved in monocyte migration and neutrophil recruitment (see reference 30 for a review). Increased mRNA expression was found for the α-chemokines ENA-78, GROα, GROβ, GROγ, and IL-8 and the β-chemokines MCP-1, MIP-1α, and MIP-1β. This is the first evidence of HZ-dependent production of ENA-78, GROα, GROβ, and GROγ in phagocytes, while few data are available for HZ effects on the expression of other chemokines in human or murine models. Increased expression of IL-8, MCP-1, and MIP-1α was previously described in HZ-fed human placental macrophages and peripheral blood monocytes (60); additionally, HZ-laden murine bone marrow and peritoneal macrophages showed enhanced expression of MCP-1, MIP-1α, and MIP-1β (23, 60). Recently, both MCP-1 and IL-8 have been related to prevention of apoptosis through activation of the NF-κB transcription system (12, 34, 62). Additionally, GROα and IL-8 are powerful triggers for firm adhesion of monocytes to the vascular endothelium, revealing an unexpected role for these chemokines in monocyte recruitment (14, 21). MCP-1 expression appears to be an important component of monocyte extravasation through the vascular endothelium (14, 69), suggesting a potential role during CM, the encephalopathy caused by massive sequestration of parasitized RBCs in the brain capillaries and associated with elevated plasma TNF-α levels, disruption of endothelial intercellular junctions and basal lamina, ring hemorrhages, and Dürck's granulomas infiltrated with macrophages (1, 31, 15, 41, 61). Since cleavage of IL-8 (as well as ENA-78) proform by MMP-9 is required for chemokine activation (65, 67) and MMP-9 involvement in CM has been proposed recently (49, 66), the role of HZ-enhanced MMP-9 effects on chemokine proform processing should be considered in future studies on CM.

HZ contains large amounts of hydroxyl (OH)-PUFAs, stable derivatives of PUFA peroxidation occurring through heme autocatalysis carried out by the polyheme moiety of highly concentrated HZ under acidic conditions (55). Six HETE isomers and two major isomers of HODE (a linoleic acid derivative) were found in HZ (55). Of these molecules and isomers, only the arachidonic acid-derived HETE isoforms mimicked the toxic effects of HZ/trophozoite phagocytosis in monocytes, such as inhibition of oxidative burst and inhibition of differentiation and maturation of monocytes into dendritic cells (63), while linoleic acid products (HODE isomers) were inactive. Ten micromolar is a reasonable approximation of the HZ-derived HETE concentration in an HZ-fed monocyte under the assumption of phagocytosis of 10 RBC equivalents of heme content per monocyte and a monocyte volume of 500 fl (55). It has been shown that 0.1 to 10 μM 15-HETE recapitulated HZ effects on IL-1β, TNF-α, and MMP-9, while lipid-free beta-hematin and dHZ did not (45–47). Here, 15-HETE effects on HZ-related chemokines were studied. Ten micromolar 15-HETE promoted transcription of ENA-78, GROα, GROβ, and IL-8. This suggests a new role for 15-HETE in HZ-dependent upregulation of these chemokines. On the other hand, chemokine (GROγ, MCP-1, MIP-1α, and MIP-1β) and cytokine (IL-1RA) expression was not affected by any dose of 15-HETE. In a murine model, both chemokines (MCP-1 and MIP-1α) were upregulated in macrophages fed with either lipid-free or native HZ, confirming that lipids are irrelevant in upregulating MCP-1 and MIP-1α via HZ (23). Interestingly, these data also fit with our present results obtained after treatment with delipidized HZ, which enhanced MCP-1 and MIP-1α gene expression (not shown). Finally, 15-HETE has been reported to have antiapoptotic properties in several studies (33, 39, 64, 68).

Both oxidative stress and cytokines have the potential to regulate the expression of HSPs, molecules that play an important role in apoptosis regulation, where they function as chaperones for denatured proteins (see references 5 and 70 for reviews). In particular, HSP27 has often been related to protection from apoptosis; additionally, HSP70 is generally referred to as an antiapoptotic molecule (3, 10, 11, 22, 29). The data presented here showed that phagocytosis of HZ enhanced HSP27, but not HSP70, protein expression. Interestingly, increased levels of HSP27 have been shown to be dependent on chemokines, such as IL-8 (51) and MIP-1β (19). It is well known that induction of HSP genes is regulated by a stress-activated transcription factor (HSF), which binds to *cis*-acting heat shock response elements (HRE), comprising multiple adjacent inverted arrays of the pentameric binding site (42). Nagarsekar et al. speculated that α-chemokines could be a new class of stress-responsive genes, as they share a promoter organization in which multiple copies of HREs are present in the 5′ upstream flanking region of each of these genes (37).

Monocyte survival can be promoted through several mechanisms, including the NF-κB transcription system and the monocyte-activated protein kinase (MAPK) cascade, whose major subfamilies are Erk, p38 MAPK, and JNK (see reference 20 for a review). Activation of the NF-κB pathway by HZ has been proposed recently in two models: in human monocytes, it has been suggested to be responsible for enhancement of TNF-α, IL-1β, and MMP-9 after phagocytosis of native, but not synthetic, HZ (47), while in murine macrophages fed with either native or synthetic HZ (beta-hematin), the activated transcription system was related to higher levels of MCP-1, MIP-1α, and MIP-1β chemokines (23). Additionally, NF-κB-mediated induction of antiapoptotic IL-8 has been reported (12). On the other hand, activation of the Erk1/2 pathway has been described in native and beta-hematin-fed murine macrophages (23, 24) but not yet in humans. However, since large amounts of data from several models indicate a correlation between activation of p38 MAPK and higher levels of IL-8 and HSP27 (2, 26, 50), major investigations into the role of MAPK cascades in HZ-dependent enhancement of chemokine expression, induction of HSP27 expression, and prevention of apoptosis is certainly warranted.

Based on the present data, the following sequence of events

occurring after phagocytosis of HZ is likely. First, 15-HETE, and most likely all HETE isoforms, induces early production of IL-1β, rapidly sustained by TNF, MMP-9, IL-1RA, and anti-apoptotic chemokine production. Therefore, as a consequence of excessive inflammation and lipoperoxidation, antiapoptotic HSP27 expression is upregulated. Finally, long-term survival of impaired monocytes is promoted. A clear understanding of the mechanisms by which HZ promotes HSP27 expression and the ensuing apoptosis block is required in a reasonable perspective to contrast the pathological persistence of circulating impaired monocytes, which might be detrimentally instrumental in inducing the hallmarks of CM. Additionally, extensive knowledge of molecules induced by HZ might be useful for the introduction of novel targeted therapies aimed at reducing cytokine-triggered disease progression toward severe malaria.

REFERENCES

1. **Aikawa, M., M. Suzuki, and Y. Gutierrez.** 1980. Pathology of malaria, p. 47. *In* J. P. Kreier (ed.), Malaria, vol. 2. Pathology, vector studies, and culture. Academic Press, New York, NY.
2. **Alford, K., S. Glennie, B. Turrell, L. Rawlinson, J. Saklatvala, and J. Dean.** 2007. Heat shock protein 27 functions in inflammatory gene expression and transforming growth factor-beta-activated kinase-1 (TAK1)-mediated signaling. J. Biol. Chem. **282**:6232–6241.
3. **Bruey, J., C. Ducasse, P. Bonniaud, L. Ravagnan, S. Susin, C. Diaz-Latoud, S. Gurbuxani, A. Arrigo, G. Kroemer, E. Solary, and C. Garrido.** 2000. Hsp27 negatively regulates cell death by interacting with cytochrome c. Nat. Cell Biol. **2**:645–652.
4. **Bzowska, M., K. Guzik, K. Barczyk, M. Ernst, H. Flad, and J. Pryjma.** 2002. Increased IL-10 production during spontaneous apoptosis of monocytes. Eur. J. Immunol. **32**:2011–2020.
5. **Christians, E., L. Yan, and I. Benjamin.** 2002. Heat shock factor 1 and heat shock proteins: critical partners in protection against acute cell injury. Crit. Care Med. **30**:S43–S50.
6. **Clark, I., A. Budd, L. Alleva, and W. Cowden.** 2006. Human malarial disease: a consequence of inflammatory cytokine release. Malar. J. **5**:85.
7. **Day, N., T. Hien, T. Schollaardt, P. Loc, L. Chuong, T. Chau, N. Mai, N. Phu, D. Sinh, N. White, and M. Ho.** 1999. The prognostic and pathophysiologic role of pro- and antiinflammatory cytokines in severe malaria. J. Infect. Dis. **180**:1288–1297.
8. **Fiori, P., P. Rappelli, S. Mirkarimi, H. Ginsburg, P. Cappuccinelli, and F. Turrini.** 1993. Reduced microbicidal and anti-tumour activities of human monocytes after ingestion of Plasmodium falciparum-infected red blood cells. Parasite Immunol. **15**:647–655.
9. **Flad, H., E. Grage-Griebenow, F. Petersen, B. Scheuerer, E. Brandt, J. Baran, J. Pryjma, and M. Ernst.** 1999. The role of cytokines in monocyte apoptosis. Pathobiology **67**:291–293.
10. **Garrido, C., J. Bruey, A. Fromentin, A. Hammann, A. Arrigo, and E. Solary.** 1999. HSP27 inhibits cytochrome c-dependent activation of procaspase-9. FASEB J. **13**:2061–2070.
11. **Garrido, C., M. Brunet, C. Didelot, Y. Zermati, E. Schmitt, and G. Kroemer.** 2006. Heat shock proteins 27 and 70: anti-apoptotic proteins with tumorigenic properties. Cell Cycle **5**:2592–2601.
12. **Garrouste, F., M. Remacle-Bonnet, C. Fauriat, J. Marvaldi, J. Luis, and G. Pommier.** 2002. Prevention of cytokine-induced apoptosis by insulin-like growth factor-I is independent of cell adhesion molecules in HT29-D4 colon carcinoma cells—evidence for a NF-kappaB-dependent survival mechanism. Cell Death Differ. **9**:768–779.
13. **Genrich, G., J. Guarner, C. Paddock, W. Shieh, P. Greer, J. Barnwell, and S. Zaki.** 2007. Fatal malaria infection in travelers: novel immunohistochemical assays for the detection of Plasmodium falciparum in tissues and implications for pathogenesis. Am. J. Trop. Med. Hyg. **76**:251–259.
14. **Gerszten, R., E. Garcia-Zepeda, Y. Lim, M. Yoshida, H. Ding, M. J. Gimbrone, A. Luster, F. Luscinskas, and A. Rosenzweig.** 1999. MCP-1 and IL-8 trigger firm adhesion of monocytes to vascular endothelium under flow conditions. Nature **398**:718–723.
15. **Gimenez, F., S. Barraud de Lagerie, C. Fernandez, P. Pino, and D. Mazier.** 2003. Tumor necrosis factor alpha in the pathogenesis of cerebral malaria. Cell Mol. Life Sci. **60**:1623–1635.
16. **Giribaldi, G., D. Ulliers, F. Mannu, P. Arese, and F. Turrini.** 2001. Growth of Plasmodium falciparum induces stage-dependent haemichrome formation, oxidative aggregation of band 3, membrane deposition of complement and antibodies, and phagocytosis of parasitized erythrocytes. Br. J. Haematol. **113**:492–499.
17. **Giribaldi, G., D. Ulliers, E. Schwarzer, I. Roberts, W. Piacibello, and P. Arese.** 2004. Hemozoin- and 4-hydroxynonenal-mediated inhibition of erythropoiesis. Possible role in malarial dyserythropoiesis and anemia. Haematologica **89**:492–493.
18. **Grau, G., T. Taylor, M. Molyneux, J. Wirima, P. Vassalli, M. Hommel, and P. Lambert.** 1989. Tumor necrosis factor and disease severity in children with falciparum malaria. N. Engl. J. Med. **320**:1586–1591.
19. **Hildebrandt, B., D. Schoeler, F. Ringel, T. Kerner, P. Wust, H. Riess, and F. Schriever.** 2006. Differential gene expression in peripheral blood lymphocytes of cancer patients treated with whole body hyperthermia and chemotherapy: a pilot study. Int. J. Hyperthermia **22**:625–635.
20. **Hunter, M., Y. Wang, T. Eubank, C. Baran, P. Nana-Sinkam, and C. Marsh.** 2009. Survival of monocytes and macrophages and their role in health and disease. Front. Biosci. **14**:4079–4102.
21. **Huo, Y., C. Weber, S. Forlow, M. Sperandio, J. Thatte, M. Mack, S. Jung, D. Littman, and K. Ley.** 2001. The chemokine KC, but not monocyte chemoattractant protein-1, triggers monocyte arrest on early atherosclerotic endothelium. J. Clin. Invest. **108**:1307–1314.
22. **Jäättelä, M.** 1999. Escaping cell death: survival proteins in cancer. Exp. Cell Res. **248**:30–43.
23. **Jaramillo, M., M. Godbout, and M. Olivier.** 2005. Hemozoin induces macrophage chemokine expression through oxidative stress-dependent and -independent mechanisms. J. Immunol. **174**:475–484.
24. **Jaramillo, M., D. Gowda, D. Radzioch, and M. Olivier.** 2003. Hemozoin increases IFN-gamma-inducible macrophage nitric oxide generation through extracellular signal-regulated kinase- and NF-kappa B-dependent pathways. J. Immunol. **171**:4243–4253.
25. **John, C., G. Park, N. Sam-Agudu, R. Opoka, and M. Boivin.** 2008. Elevated serum levels of IL-1ra in children with Plasmodium falciparum malaria are associated with increased severity of disease. Cytokine **41**:204–208.
26. **Kim, Y., M. Song, and J. Ryu.** 2009. Inflammation in methotrexate-induced pulmonary toxicity occurs via the p38 MAPK pathway. Toxicology **256**:183–190.
27. **Kwiatkowski, D.** 1990. Tumour necrosis factor, fever and fatality in falciparum malaria. Immunol. Lett. **25**:213–216.
28. **Laemmli, U.** 1970. Cleavage of structural proteins during the assembly of the head of bacteriophage T4. Nature **227**:680–685.
29. **Lanneau, D., A. de Thonel, S. Maurel, C. Didelot, and C. Garrido.** 2007. Apoptosis versus cell differentiation: role of heat shock proteins HSP90, HSP70 and HSP27. Prion **1**:53–60.
30. **Luster, A.** 1998. Chemokines—chemotactic cytokines that mediate inflammation. N. Engl. J. Med. **338**:436–445.
31. **Medana, I. M., and G. D. Turner.** 2006. Human cerebral malaria and the blood-brain barrier. Int. J. Parasitol. **36**:555–568.
32. **Mordmüller, B., F. Turrini, H. Long, P. Kremsner, and P. Arese.** 1998. Neutrophils and monocytes from subjects with the Mediterranean G6PD variant: effect of Plasmodium falciparum hemozoin on G6PD activity, oxidative burst and cytokine production. Eur. Cytokine Netw. **9**:239–245.
33. **Moreno, C.** 2009. New aspects of the role of hydroxyeicosatetraenoic acids in cell growth and cancer development. Biochem. Pharmacol. **77**:1–10.
34. **Morimoto, H., M. Hirose, M. Takahashi, M. Kawaguchi, H. Ise, P. Kolattukudy, M. Yamada, and U. Ikeda.** 2008. MCP-1 induces cardioprotection against ischaemia/reperfusion injury: role of reactive oxygen species. Cardiovasc. Res. **78**:554–562.
35. **Mosser, D., and R. Morimoto.** 2004. Molecular chaperones and the stress of oncogenesis. Oncogene **23**:2907–2918.
36. **Mujuzi, G., B. Magambo, B. Okech, and T. G. Egwang.** 2006. Pigmented monocytes are negative correlates of protection against severe and complicated malaria in Ugandan children. Am. J. Trop. Med. Hyg. **74**:724–729.
37. **Nagarsekar, A., J. Hasday, and I. Singh.** 2005. CXC chemokines: a new family of heat-shock proteins? Immunol. Invest. **34**:381–398.
38. **Nagase, H., and J. J. Woessner.** 1999. Matrix metalloproteinases. J. Biol. Chem. **274**:21491–21494.
39. **Nishio, E., and Y. Watanabe.** 1997. The regulation of mitogenesis and apoptosis in response to the persistent stimulation of alpha1-adrenoceptors: a possible role of 15-lipoxygenase. Br. J. Pharmacol. **122**:1516–1522.
40. **Odeh, M.** 2001. The role of tumour necrosis factor-alpha in the pathogenesis of complicated falciparum malaria. Cytokine **14**:11–18.

41. **Patnaik, J., B. Das, S. Mishra, S. Mohanty, S. Satpathy, and D. Mohanty.** 1994. Vascular clogging, mononuclear cell margination, and enhanced vascular permeability in the pathogenesis of human cerebral malaria. Am. J. Trop. Med. Hyg. **51:**642–647.

42. **Perisic, O., H. Xiao, and J. Lis.** 1989. Stable binding of Drosophila heat shock factor to head-to-head and tail-to-tail repeats of a conserved 5 bp recognition unit. Cell **59:**797–806.

43. **Pfaffl, M. W.** 2001. A new mathematical model for relative quantification in real-time RT-PCR. Nucleic Acids Res. **29:**2002–2007.

44. **Pichyangkul, S., P. Saengkrai, and H. Webster.** 1994. Plasmodium falciparum pigment induces monocytes to release high levels of tumor necrosis factor-alpha and interleukin-1 beta. Am. J. Trop. Med. Hyg. **51:**430–435.

45. **Prato, M., V. Gallo, and P. Arese.** 2010. Higher production of tumor necrosis factor alpha in hemozoin-fed human adherent monocytes is dependent on lipidic component of malarial pigment: new evidences on cytokine regulation in Plasmodium falciparum malaria. Asian Pac. J. Trop. Med. **3:**85–89.

46. **Prato, M., V. Gallo, G. Giribaldi, and P. Arese.** 2008. Phagocytosis of haemozoin (malarial pigment) enhances metalloproteinase-9 activity in human adherent monocytes: Role of IL-1beta and 15-HETE. Malar. J. **7:**157.

47. **Prato, M., V. Gallo, G. Giribaldi, E. Aldieri, and P. Arese.** Role of the NF-κB transcription pathway in the hemozoin- and 15-HETE-mediated activation of matrix metalloproteinase-9 in human adherent monocytes. Cell. Microbiol., in press. doi:10.1111/j.1462-5822.2010.01508.x.

48. **Prato, M., G. Giribaldi, and P. Arese.** 2009. Hemozoin triggers tumor necrosis factor alpha-mediated release of lysozyme by human adherent monocytes: new evidences on leukocyte degranulation in P. falciparum malaria. Asian Pac. J. Trop. Med. **2:**35–40.

49. **Prato, M., G. Giribaldi, M. Polimeni, V. Gallo, and P. Arese.** 2005. Phagocytosis of hemozoin enhances matrix metalloproteinase-9 activity and TNF-alpha production in human monocytes: role of matrix metalloproteinases in the pathogenesis of falciparum malaria. J. Immunol. **175:**6436–6442.

50. **Rajaiya, J., J. Xiao, R. Rajala, and J. Chodosh.** 2008. Human adenovirus type 19 infection of corneal cells induces p38 MAPK-dependent interleukin-8 expression. Virol. J. **5:**17.

51. **Rane, M., Y. Pan, S. Singh, D. Powell, R. Wu, T. Cummins, Q. Chen, K. McLeish, and J. Klein.** 2003. Heat shock protein 27 controls apoptosis by regulating Akt activation. J. Biol. Chem. **278:**27828–27835.

52. **Schrimpe, A., and D. Wright.** 2009. Differential gene expression mediated by 15-hydroxyeicosatetraenoic acid in LPS-stimulated RAW 264.7 cells. Malar. J. **8:**195.

53. **Schwarzer, E., M. Alessio, D. Ulliers, and P. Arese.** 1998. Phagocytosis of the malarial pigment, hemozoin, impairs expression of major histocompatibility complex class II antigen, CD54, and CD11c in human monocytes. Infect. Immun. **66:**1601–1606.

54. **Schwarzer, E., G. Bellomo, G. Giribaldi, D. Ulliers, and P. Arese.** 2001. Phagocytosis of malarial pigment haemozoin by human monocytes: a confocal microscopy study. Parasitology **123:**125–131.

55. **Schwarzer, E., H. Kuhn, E. Valente, and P. Arese.** 2003. Malaria-parasitized erythrocytes and hemozoin nonenzymatically generate large amounts of hydroxy fatty acids that inhibit monocyte functions. Blood **101:**722–728.

56. **Schwarzer, E., O. Skorokhod, V. Barrera, and P. Arese.** 2008. Hemozoin and the human monocyte—a brief review of their interactions. Parassitologia **50:**143–145.

57. **Schwarzer, E., F. Turrini, and P. Arese.** 1994. A luminescence method for the quantitative determination of phagocytosis of erythrocytes, of malaria-parasitized erythrocytes and of malarial pigment. Br. J. Haematol. **88:**740–745.

58. **Schwarzer, E., F. Turrini, D. Ulliers, G. Giribaldi, H. Ginsburg, and P. Arese.** 1992. Impairment of macrophage functions after ingestion of Plasmodium falciparum-infected erythrocytes or isolated malarial pigment. J. Exp. Med. **176:**1033–1041.

59. **Scorza, T., S. Magez, L. Brys, and P. De Baetselier.** 1999. Hemozoin is a key factor in the induction of malaria-associated immunosuppression. Parasite Immunol. **21:**545–554.

60. **Sherry, B., G. Alava, K. Tracey, J. Martiney, A. Cerami, and A. Slater.** 1995. Malaria-specific metabolite hemozoin mediates the release of several potent endogenous pyrogens (TNF, MIP-1 alpha, and MIP-1 beta) in vitro, and altered thermoregulation in vivo. J. Inflamm. **45:**85–96.

61. **Silamut, K., N. Phu, C. Whitty, G. Turner, K. Louwrier, N. Mai, J. Simpson, T. Hien, and N. White.** 1999. A quantitative analysis of the microvascular sequestration of malaria parasites in the human brain. Am. J. Pathol. **155:**395–410.

62. **Singh, R., and B. Lokeshwar.** 2009. Depletion of intrinsic expression of Interleukin-8 in prostate cancer cells causes cell cycle arrest, spontaneous apoptosis and increases the efficacy of chemotherapeutic drugs. Mol. Cancer **8:**57.

63. **Skorokhod, O., M. Alessio, B. Mordmüller, P. Arese, and E. Schwarzer.** 2004. Hemozoin (malarial pigment) inhibits differentiation and maturation of human monocyte-derived dendritic cells: a peroxisome proliferator-activated receptor-gamma-mediated effect. J. Immunol. **173:**4066–4074.

64. **Tang, D., Y. Chen, and K. Honn.** 1996. Arachidonate lipoxygenases as essential regulators of cell survival and apoptosis. Proc. Natl. Acad. Sci. U. S. A. **93:**5241–5246.

65. **Van den Steen, P., P. Proost, A. Wuyts, J. Van Damme, and G. Opdenakker.** 2000. Neutrophil gelatinase B potentiates interleukin-8 tenfold by aminoterminal processing, whereas it degrades CTAP-III, PF-4, and GRO-alpha and leaves RANTES and MCP-2 intact. Blood **96:**2673–2681.

66. **Van den Steen, P., I. Van Aelst, S. Starckx, K. Maskos, G. Opdenakker, and A. Pagenstecher.** 2006. Matrix metalloproteinases, tissue inhibitors of MMPs and TACE in experimental cerebral malaria. Lab. Invest. **86:**873–888.

67. **Van Den Steen, P., A. Wuyts, S. Husson, P. Proost, J. Van Damme, and G. Opdenakker.** 2003. Gelatinase B/MMP-9 and neutrophil collagenase/MMP-8 process the chemokines human GCP-2/CXCL6, ENA-78/CXCL5 and mouse GCP-2/LIX and modulate their physiological activities. Eur. J. Biochem. **270:**3739–3749.

68. **Wang, S., Y. Wang, J. Jiang, R. Wang, L. Li, Z. Qiu, H. Wu, and D. Zhu.** 2010. 15-HETE protects rat pulmonary arterial smooth muscle cells from apoptosis via the PI3K/Akt pathway. Prostaglandins Other Lipid Mediat. **91:**51–60.

69. **Weber, K., P. von Hundelshausen, I. Clark-Lewis, P. Weber, and C. Weber.** 1999. Differential immobilization and hierarchical involvement of chemokines in monocyte arrest and transmigration on inflamed endothelium in shear flow. Eur. J. Immunol. **29:**700–712.

70. **Yenari, M., J. Liu, Z. Zheng, Z. Vexler, J. Lee, and R. Giffard.** 2005. Anti-apoptotic and anti-inflammatory mechanisms of heat-shock protein protection. Ann. N. Y. Acad. Sci. **1053:**74–83.

Editor: J. H. Adams